

2 **Determination of black carbon mass concentration from aerosol light** 3 **absorption using variable mass absorption cross-section**

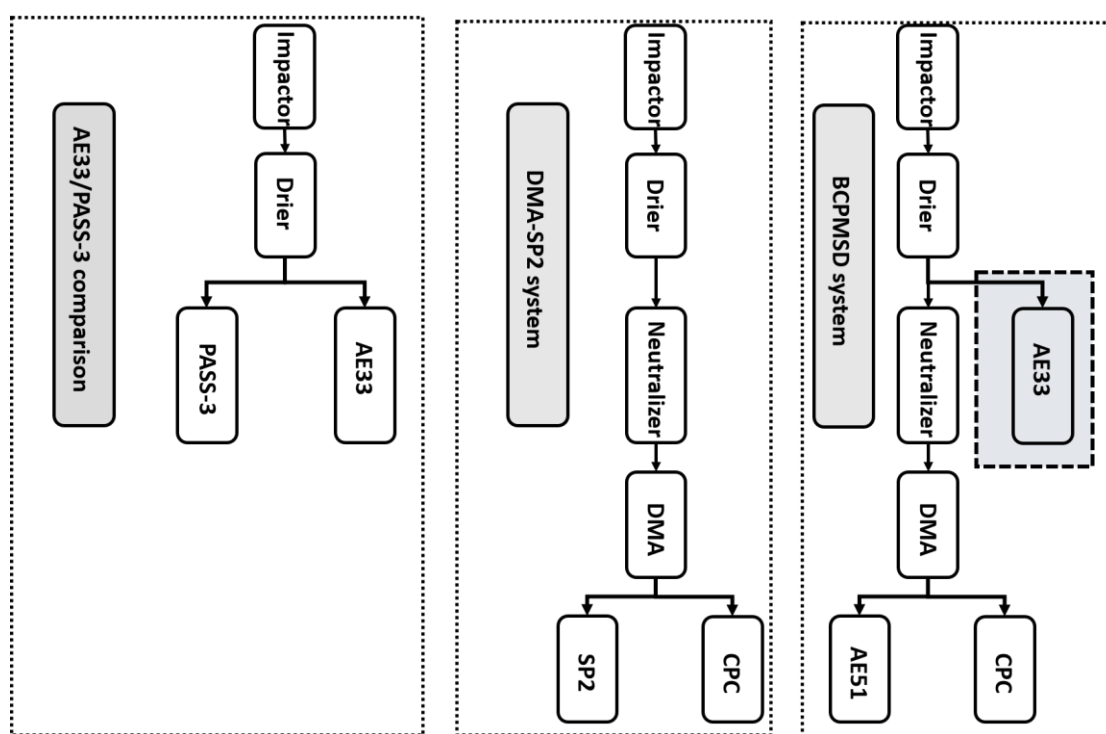
4 Weilun Zhao¹, Wangshu Tan¹, Gang Zhao², Chuanyang Shen¹, Yingli Yu¹, Chunsheng Zhao¹

5 ¹Department of Atmospheric and Oceanic Sciences, School of Physics, Peking University, Beijing 100871, China

6 ²State Key Joint Laboratory of Environmental Simulation and Pollution Control, College of Environmental Sciences and
 7 Engineering, Peking University, Beijing 100871, China

8

9 **1 The schematic representation of the three different measurement systems**



10

11 **Figure S1. The schematic diagram of the AE33/PASS-3 comparison system, DMA-SP2 system and BCPMSD measurement**
 12 **system.**

13 **2 The uncertainties of derived BC mass concentration caused by using a constant BC-containing particle fraction**

14 Figure.S2 shows the deviation of BC particle mass size distribution (BCPMSD) calculated from different BC-containing particle
 15 fractions (8.5%, 17%, 34%). We can see that for our newly proposed method, using a constant BC-containing particle fraction does
 16 not change the size-resolved distribution mode. There is still a finer mode and coarser mode with a boundary of 240 nm. Besides,
 17 the influence of using different BC-containing particle fractions to derived BC mass concentration (m_{BC}) is very limited when
 18 particles are larger than 200 nm. However, the deviations between the m_{BC} derived from different fraction values are large when
 19 particles diameters are smaller than 200 nm. At this range, if the BC-containing particle fraction is underestimated, the m_{BC} will be
 20 underestimated. On the contrary, the m_{BC} is overestimated if the fraction is overestimated.

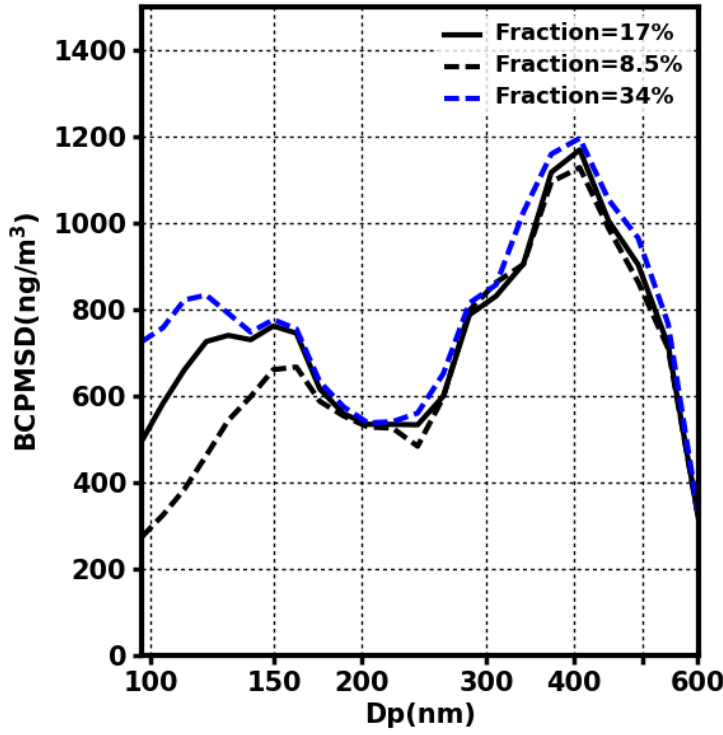


Figure S2. The derived BCPMSD by using different constant BC-containing particle fraction. The solid black line represents the result derived from a fraction of 17%. The dashed black line and blue line show the results derived from a fraction of half of 8.5% and double of 34%.

3 The uncertainties of MAC caused by using idealized core-shell model

3.1 The formation of BC aggregates with a determined morphology

The fractal aggregates of BC have been well described by fractal geometries through the well-known statistical scaling law (Sorensen, 2001):

$$N = k_f \left(\frac{R_g}{a} \right)^{D_f}, \quad (1)$$

where N is the number of “same-sized” monomers in the cluster, a is the monomer radius, D_f and k_f are known as the fractal dimension and fractal prefactor respectively, determining the morphology of BC cluster. The compactness of a fractal aggregate increases as the increase of D_f or k_f . R_g is the gyration radius, inferring the overall aggregate radius, determined by :

$$R_g = \sqrt{\frac{1}{N} \sum_{i=1}^N r_i^2}, \quad (2)$$

where r_i represents the distance of the i th monomer from the center of mass of BC cluster.

In order to generate fractal-like aggregates with given N , R_g , a , D_f and k_f , the sequential algorithm proposed in Filippov et al. (2000) is introduced in this paper to add the primary monomers one by one. On condition that there is an aggregate including $N-1$ monomers, the N th monomer is constantly placed randomly until it has at least one contact point with the previously attached $N-1$ monomers with no overlapping. Besides, the mass center of the next N th monomer must obey the rule as follows:

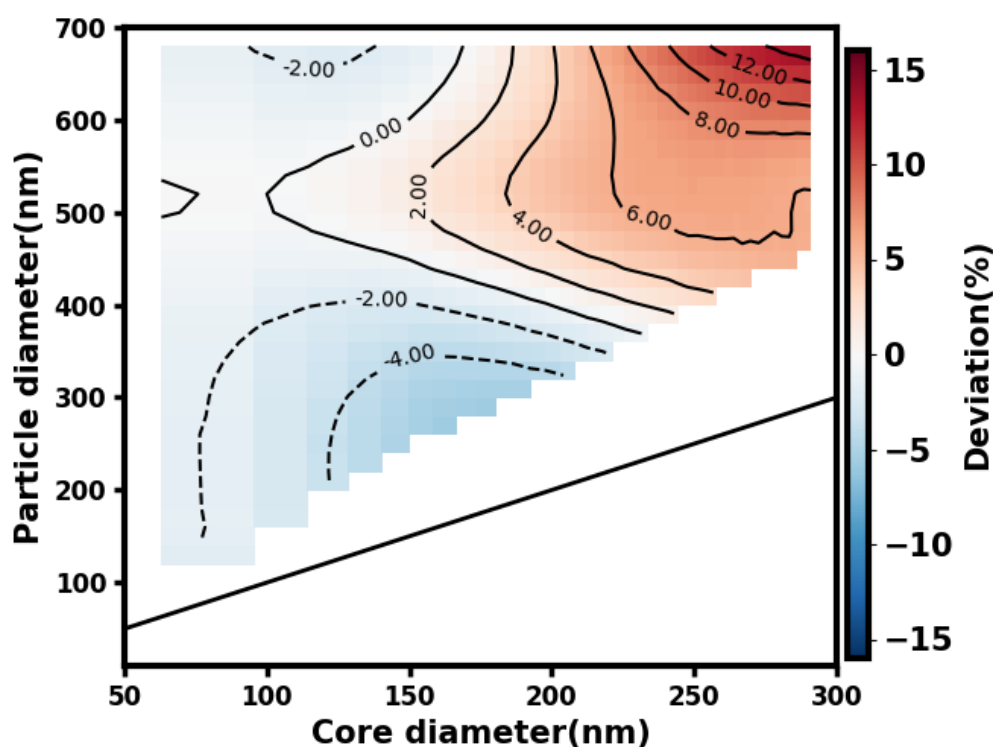
$$(r_N - r_{N-1})^2 = \frac{N^2 a^2}{N-1} \left(\frac{N}{k_f} \right)^{2/D_f} - \frac{N a^2}{N-1} - N a^2 \left(\frac{N-1}{k_f} \right)^{2/D_f}, \quad (3)$$

40 where r_{N-1} and r_N are the mass center of the first N-1 monomers and the Nth monomer, respectively. After the fractal
41 configuration of BC aggregates, the absorption properties of BC containing particles need to be evaluate.

42 The fractal dimensions for aged BC aggregates are generally close to 3 (Kahnert et al., 2012). The aim of this study is to evaluate
43 the effects of aerosol microphysics on the absorption enhancement of fully coated BC particles, which can be regarded as the aged
44 BC aerosols. Therefore, the fractal dimension D_f is set to be 2.8 and k_f is generally set to be 1.2. The diameter of the primary
45 monomers are usually between 20-50 nm and the number of the primary monomers for an aggregates is between 50-300. The size
46 of BC core calculated by the new method is smaller than 300 nm most of the time during Zhangqiu campaign. The diameter of
47 primary monomers is set to be 50 nm and the number of the primary monomers for an aggregates ranges from 2 to 200, leading to
48 the largest size of volume equivalent BC core close to 300 nm. Summary results indicate that the real part of BC is generally in the
49 range of 1.5 to 2.0 while the imaginary part usually varies from 0.5 to 1.1 (Liu et al., 2018). Therefore, the mean value 1.75 for BC
50 real part and 0.8 for BC imaginary part are adopted here to calculate MAC values for BC/sulfate mixtures at the wavelength of 880
51 nm.

52 3.2 Multiple Sphere T-matrix (MSTM) method

53 As the traditional Mie model is not available for the fractal aggregates, the widely used MSTM method is employed here to quantify
54 the absorption properties of BC clusters (Mackowski and Mishchenko, 1996;Mackowski, 2014). The addition theorem of vector
55 spherical wave functions is used in MSTM method to describe the mutual interactions among the system. The T-matrix of aggregates
56 used to derive particle optical properties can be obtained from these individual monomers. MSTM method can calculate light
57 scattering and absorption properties of the randomly oriented aggregates without numerical averaging over particle orientations if
58 the position, size and refractive index of every spherical element are given. However, the MSTM method is only applicable to
59 evaluate the aggregates of spheres without overlapping and it is carried out with high computational demand.



61 **Figure S3. Relative deviations of MAC values calculated by idealized concentric core-shell model and letting BC particles**
62 **be in the form of cluster-like aggregates. The solid line is 1:1 line.**

63 The deviations showed in Fig.S3 are derived by subtracting MAC values calculated by MSTM model by those calculated by Mie
64 model. The results indicate that most of the MAC values calculated by assuming BC particles are in the form of cluster-like
65 aggregates are smaller when the size of BC core is smaller than 150 nm. When BC core is larger than 150 nm, the MAC values
66 calculated by MSTM model increase with the thickness of shell and will be larger than those derived from concentric core-shell
67 model. As we can see from Fig.S3, the deviations between MAC calculated by the idealized concentric core-shell model and letting
68 BC particles be in the form of cluster-like aggregates are within 15%.

69 **References**

- 70 Filippov, A. V., Zurita, M., and Rosner, D. E.: Fractal-like aggregates: Relation between morphology and physical properties, *J.*
71 *Colloid Interface Sci.*, 229, 261-273, 10.1006/jcis.2000.7027, 2000.
- 72 Kahnert, M., Nousiainen, T., Lindqvist, H., and Ebert, M.: Optical properties of light absorbing carbon aggregates mixed with sulfate:
73 assessment of different model geometries for climate forcing calculations, *Optics Express*, 20, 17, 10.1364/oe.20.010042, 2012.
- 74 Liu, C., Chung, C. E., Yin, Y., and Schnaiter, M.: The absorption Angstrom exponent of black carbon: from numerical aspects,
75 *Atmospheric Chemistry and Physics*, 18, 6259-6273, 10.5194/acp-18-6259-2018, 2018.
- 76 Mackowski, D. W., and Mishchenko, M. I.: Calculation of the T matrix and the scattering matrix for ensembles of spheres, *J. Opt.*
77 *Soc. Am. A-Opt. Image Sci. Vis.*, 13, 2266-2278, 10.1364/josaa.13.002266, 1996.
- 78 Mackowski, D. W.: A general superposition solution for electromagnetic scattering by multiple spherical domains of optically active
79 media, *Journal of Quantitative Spectroscopy & Radiative Transfer*, 133, 264-270, 10.1016/j.jqsrt.2013.08.012, 2014.
- 80 Sorensen, C. M.: Light scattering by fractal aggregates: A review, *Aerosol Science and Technology*, 35, 648-687,
81 10.1080/027868201316900007, 2001.